1-1-2008

Temperature-dependent spectroscopic properties of Tm(3+) in germanate, silica, and phosphate glasses: A comparative study

Giorgio Turri
University of Central Florida

Vikas Sudesh
University of Central Florida

Martin Richardson
University of Central Florida

Michael Bass
University of Central Florida

Alessandra Toncelli

Temperature-dependent spectroscopic properties of Tm^{3+} in germanate, silica, and phosphate glasses: A comparative study

Cite as: J. Appl. Phys. **103**, 093104 (2008); https://doi.org/10.1063/1.2912952
Submitted: 31 December 2007 . Accepted: 25 February 2008 . Published Online: 06 May 2008

Giorgio Turri, Vikas Sudesh, Martin Richardson, Michael Bass, Alessandra Toncelli, and Mauro Tonelli

Temperature-dependent spectroscopic properties of Tm^{3+} in germanate, silica, and phosphate glasses: A comparative study

Giorgio Turri,[1,a)] Vikas Sudesh,[1] Martin Richardson,[1] Michael Bass,[1] Alessandra Toncelli,[2] and Mauro Tonelli[2]
[1]*CREOL, The College of Optics and Photonics, University of Central Florida, Orlando, Florida 32816, USA*
[2]*NEST INFM-CNR, Dipartimento di Fisica, Universitá di Pisa, Largo B. Pontecorvo 3, 56127 Pisa, Italy*

(Received 31 December 2007; accepted 25 February 2008; published online 5 May 2008)

Spectroscopic properties of thulium-doped germanate, silica, and phosphate glasses were measured and compared since such glasses are of interest as materials for fiber lasers in the eye-safe wavelength region. $^3F_4$ excited state fluorescence decay dynamics was investigated at temperatures from 8 to 300 K and the results revealed a strong dependence of the $^3F_4$ lifetime on the host matrix. The temperature-dependent stimulated emission cross section was obtained by using the Fuchtbauer–Ladenburg technique. In phosphate glass the fluorescent lifetime is short, making this material difficult to use for 2 μm laser purposes. Tm^{3+}-doped germanate glass shows a longer lifetime than silica, a comparable value of stimulated emission cross section and some interesting temperature-independent properties. © *2008 American Institute of Physics*.
[DOI: 10.1063/1.2912952]

I. INTRODUCTION

Lasers based on the trivalent thulium (Tm^{3+}) $^3F_4$-$^3H_6$ transition have been successfully used in coherent radar systems, remote sensing, and medical applications.[1] The emission around 2 μm falls in the eye-safe region and phonon broadening allows for wide tunability in the 1870 –2160 nm range.[2] Tm^{3+} can be pumped to the $^3H_4$ level at around 800 nm, a wavelength easily accessible with commercially available laser diodes. If the doping concentration is high enough, the self-quenching of the $^3H_4$ decay triggers the two-for-one process[3] producing up to two atoms in the $^3F_4$ upper laser level for every absorbed pump photon and resulting in a quantum efficiency $\leqslant 2$.

In this paper we present the spectroscopic properties of Tm^{3+}-doped silica, germanate, and phosphate glasses. Silica has the advantages of high mechanical strength and high damage threshold compared to phosphate and germanate glasses. Also, it is the most commonly used material for optical fibers, and the tools to handle and splice optical fibers are designed for silica standards. On the other hand, nonradiative decay is very strong in silica due to the high phonon energy that extends to 1100 cm^{-1}.[4] In Tm:germanate[5] the phonon energy extends only to 900 cm^{-1} so this material is expected to suffer less from phonon quenching. On the contrary, Tm:phosphate has an even higher phonon energy than Tm:silica,[6] but some phosphate glasses, as the one investigated in this work, have the interesting property of a negative dn/dT, allowing the possibility of athermal designs. Also, phosphate glass has high chemical durability, high solubility for rare earth dopant ions, is only slightly sensitive to concentration quenching, and, if co-doped, has a high energy transfer rate.[7] These properties would make phosphate glass a very suitable host provided phonon quenching is not too strong.

There is an extensive literature on Tm-doped silica and silicate glasses (see, for example, Jander and Brocklesby[8] and references therein). In contrast, there are very few studies of Tm:germanate[9] and even fewer on Tm:phosphate. Those in recent years concentrate on lead germanate[10] and fluorophosphates.[11–13]

We first measured the absorption spectra of samples of each of these glasses at room temperature to obtain the radiative lifetimes by the Judd–Ofelt technique and the absolute emission cross sections at room temperature by the reciprocity method. Then, the fluorescence emission spectra were measured in the 35–300 K range, and the emission cross section as a function of temperature was obtained with the Fuchtbauer–Ladenburg (FL) technique.[14] Finally, the decay dynamics of the $^3F_4$ state was investigated at different temperatures as low as 8 K. A partial energy level diagram for Tm^{3+} is depicted in Fig. 1.

II. EXPERIMENTAL

The Tm:silica sample, provided by Nufern (Ref. 15) consisted of a SiO_2 matrix with 10.3 wt % Al_2O_3, doped with 3.45 wt % Tm_2O_3, corresponding to 2.37 $\times 10^{20}$ Tm^{3+} ions/cm^3. The Tm^{3+}:germanate and the Tm^{3+}:phosphate samples were provided by Kigre Inc.,[16] and their exact composition is propriety. Both were prepared with 4 wt % Tm_2O_3 doping, corresponding to 6.24 $\times 10^{20}$ Tm^{3+} ions/cm^3 in the germanate and 3.99 $\times 10^{20}$ Tm^{3+} ions/cm^3 in the phosphate sample. Germanium oxide is the main component of the germanate sample which also contains minor amounts of barium and zinc oxides. The phosphate sample was Kigre Q-100 an athermal borophosphate glass. When doped with Nd^{3+} ions[17] Q-100 is a useful

a)Author to whom correspondence should be addressed. Electronic mail: gturri@mail.ucf.edu.

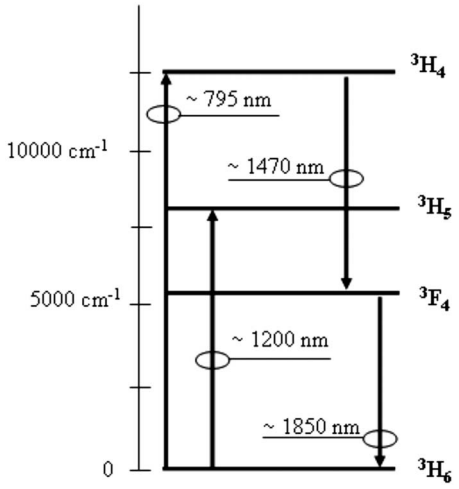

FIG. 1. Energy level scheme of trivalent thulium.

laser material. The values of the doping concentration provided by Nufern and Kigre are assumed accurate to within 10%.

The samples' transmission spectra were measured at room temperature by using a Cary 500 spectrophotometer by Varian, Inc. Spectra were collected in the 200–2300 nm range with 0.25 nm steps by using unpolarized light with the spectral bandwidth fixed to 1 nm. The transmission data were corrected for Fresnel reflection at the sample surfaces and the absorption cross section as a function of wavelength was obtained. These spectra were used to perform the Judd–Ofelt analysis.

For emission spectroscopy the samples were pumped to the $^3H_4$ level by a continuous, 1 W fiber-coupled diode laser emitting around 800 nm. The power of the pump laser was monitored during data acquisition, and the collected spectra were corrected for the pump variations which were typically less than 1%. The emitted fluorescence was measured with a NIR Ocean Optics spectrometer cooled to −15 °C. The wavelength accuracy of the spectrometer was checked in the 1.0–2.2 μm region by measuring the emission of a tunable Yb:Er laser and the first and second order peaks of a Nd:YVO_4 laser emitting at 1.064 μm. Deviations from the measured to the accepted laser wavelengths were less than 2 nm while the spectral resolution of the spectrometer was ~20 nm [full width at half maximum (FWHM)]. Although large, the spectral resolution is still acceptable in these emission measurements since the Tm^{3+} $^3F_4$-$^3H_6$ emission consists of a broad peak with about 300 nm FWHM. The wavelength dependence of the spectrometer-detector combination's sensitivity was determined by using a calibrated tungsten-quartz halogen lamp, and the results were used to correct the intensity of the measured Tm^{3+} emission spectra. For each sample, up to 20 spectra at each temperature in the 35–300 K range were collected, and the results were averaged to improve the signal-to-noise ratio.

The decay dynamics of the Tm^{3+} $^3F_4$ state was also investigated by pumping the samples to the Tm^{3+} $^3H_4$ level. Two independent sets of measurements were taken: The first for the temperature range 35–300 K and the second at temperatures between 8 and 300 K. In the first experimental apparatus a tunable laser system by Spectra Physics consisting of a parametric amplifier pumped by the third harmonic of a *Q*-switched Nd:YAG laser provided a 4 ns FWHM pulse at 795 nm with about 10 mJ/pulse energy at 10 Hz repetition rate. The emitted fluorescence was focused onto an InGaAs detector coupled to a built-in amplifier with a measured response time of ~75 ns. A long-pass RG-1000 filter transmitting wavelengths longer than 1 μm prevented any pump light from reaching the detector. The signal from the detector was measured by a 1 GHz digital oscilloscope triggered by a signal synchronized with the pump laser pulse and the fluorescence decay recorded on a computer. This apparatus was also used to investigate the dynamics of the $^3F_4$ state in the silica and phosphate samples pumped to the $^3H_5$ state around 1200 nm by replacing the RG-1000 filter with a band pass BG-18 filter transmitting in the 1600–2600 nm region. For the second set of measurements the excitation source was a Ti:sapphire laser providing a 30 ns FWHM pulse, tuned around 790 nm wavelength, with some 10 μJ/pulse energy at 10 Hz repetition rate. The emitted fluorescence was collected from a small portion (about 1 mm) of the sample and focused onto a liquid nitrogen cooled InSb detector: A silicon filter was placed in front of the detector to cut the pump light. The signal was amplified and recorded with a digital oscilloscope.

III. RESULTS

A. Absorption spectrum and Judd–Ofelt analysis

The absorption spectra from 350 to 2200 nm of 3.45% Tm:silica, 4% Tm:germanate, and 4% Tm:phosphate glasses are shown in Fig. 2. Although the absorption cross sections are different for the three samples, the positions of the peaks are similar (this is also true for the $^1D_2$ peak around 358 nm, which is not shown in Fig. 2), with the exception of a shift of the $^3F_4$ peak to longer wavelength in phosphate. In pure silica the short-wavelength absorption edge starts at 200 nm longer wavelength than in the other two hosts, extending almost under the $^3F_{2,3}$ peak.

For the Judd–Ofelt analysis, we used all the absorption peaks reported in Fig. 2, except the $^1G_4$ peak for the silica sample because of the overlap with the short-wavelength absorption edge of the host. The values of the reduced matrix elements calculated by Walsh *et al.* were used.[18,19] The resulting Judd–Ofelt parameters and radiative lifetimes are reported in Table I and compared to some of the values available in literature.[19–23] A comparison among the results published by different authors for glass samples is difficult because the optical properties of doped glasses strongly depend on the details of the composition, the fabrication, and the doping of the glass. Furthermore, in the specific case of thulium, only a few peaks can be used to fit the three Judd–Ofelt parameters, resulting in lower accuracy Judd–Ofelt results. However, some consistency can be observed in Table I. The order of the Judd–Ofelt parameters is $\Omega_2 > \Omega_4 > \Omega_6$ for Tm:germanate and Tm:silica. For Tm:phosphate, our results agree with Lakshman's in the sense that in the phosphate glass containing boron, the order of the parameters is $\Omega_2 > \Omega_6 > \Omega_4$ rather than $\Omega_2 > \Omega_4 > \Omega_6$ as it is in phosphate and

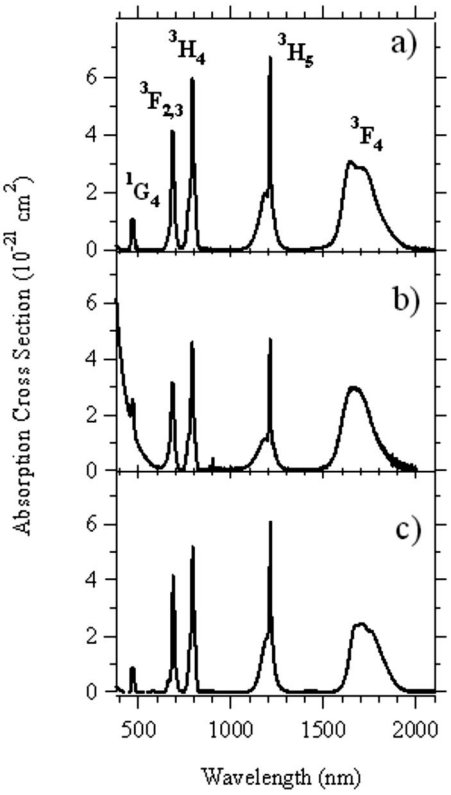

FIG. 2. Absorption spectra of (a) Tm:germanate, (b) Tm:silica, and (c) Tm:phosphate.

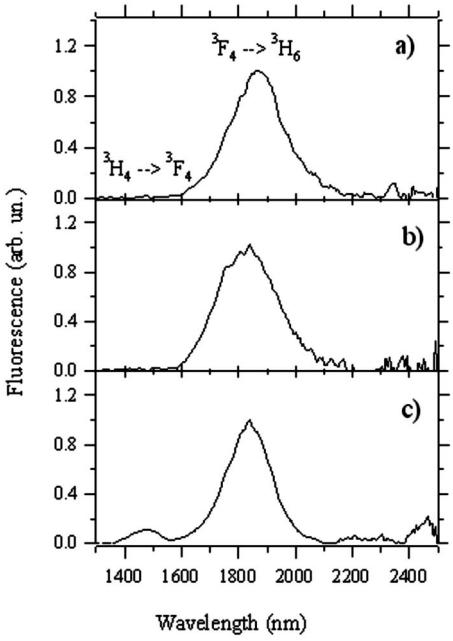

FIG. 3. Fluorescence spectra at room temperature: (a) Tm:germanate, (b) Tm:silica, and (c) Tm:phosphate. The amplitudes have been normalized to one at the peak emission wavelength (around 1850 nm). For Tm:phosphate the peak emission strength is comparable to that of the weak emission around 1470 nm.

fluorophosphate.[23] Reference 23 reports Judd–Ofelt parameters that are three times those we report which suggests that the Tm:borophosphate material they investigated was very different from the Kigre Q-100 host glass studied in this paper.

For all three materials, the calculated radiative lifetimes range between 4 and 8 ms.

B. Emission spectra at room temperature

Figure 3 shows the emission spectra of the three materials at room temperature where the fluorescence intensities have been normalized to one at the emission maximum. In Tm:germanate and Tm:silica the spectrum is dominated by the peak associated with the $^3F_4 \rightarrow {}^3H_6$ transition; in Tm:phosphate the emission around 1470 nm due to the $^3H_4 \rightarrow {}^3F_4$, transition also contributes to the spectrum. In most Tm-doped glasses the $^3H_4 \rightarrow {}^3F_4$ transition is strongly quenched.[24–26] Only in materials with very low phonon energies, such as Tm:yttria-alumina-silica glass[8] and Tm^{3+}-doped fluoride fibers[24,25] is its radiative decay strong enough for practical applications. The calculation of the emission cross section at 1470 nm and its temperature dependence would require a separate investigation that is beyond the purposes of this paper. In the remainder of this paper we shall concentrate on the $^3F_4 \rightarrow {}^3H_6$ transition only.

TABLE I. Results of Judd–Ofelt analysis and comparison with literature.

Material	Tm concentration (10^{20} ions/cm^3)	Ω_2 (10^{-20} cm^2)	Ω_4 (10^{-20} cm^2)	Ω_6 (10^{-20} cm^2)	$^3F_4$ τ_{rad} (ms)	Reference
Tm:germanate	6.24	4.4	1.2	0.9	5.3	This work
	···	4.0	1.6	0.8	···	20 and 21
	2.50	···	···	···	4.97	22
Tm:silica	2.37	3.7	2.3	0.6	7.0	This work
	···	6.23	1.91	1.36	4.56	19
	3.52	···	···	···	6.3	22
Tm:borophosphate	3.99	3.6	0.7	1	8.3	This work
	···	9.8	1.9	3.4	···	23
Tm:fluorophosphate	···	4.12	1.47	0.72	···	20 and 21
Tm:phosphate	···	5.7	3.0	0.8	···	20 and 21
	2.35	···	···	···	5.0	22

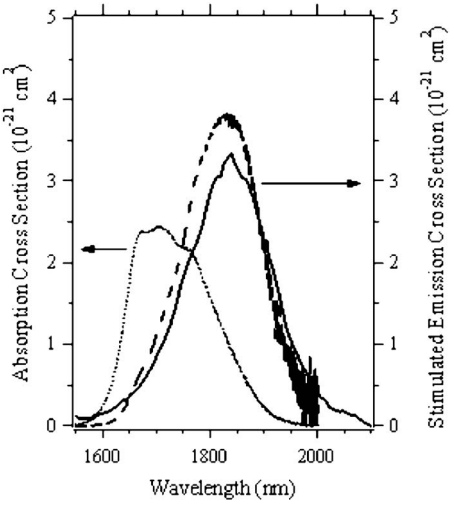

FIG. 4. Comparison of the emission cross section of Tm:phosphate at room temperature as obtained by the FL model (—) and by the reciprocity method (– –). The absorption cross section is also shown (···).

The emission cross section, $\sigma_{em}^{FL}(\lambda)$, can be obtained from the measured fluorescence spectrum, $I(\lambda)$, by using the[14] (FL) formula

$$\sigma_{em}^{FL}(\lambda) = \frac{\lambda^5 \beta}{8\pi c n^2 \tau_{rad}} \frac{I(\lambda)}{\int \lambda I(\lambda) d\lambda}, \quad (1)$$

where n is the refractive index of the sample, c is the speed of light, and β is the branching ratio (for the $^3F_4$ level, $\beta = 1$) provided that the radiative lifetime τ_{rad} is known. Usually the latter is obtained either by the Judd–Ofelt technique or by measuring the fluorescence lifetime τ_{fluo} at temperature close to absolute zero. A different approach is to evaluate the emission cross section from the measured absorption cross section $\sigma_{abs}(\lambda)$ with the so-called reciprocity formula[14]

$$\sigma_{em}^{rec}(\lambda) = \sigma_{abs}(\lambda) \frac{Z_l}{Z_u} \exp\left[\frac{E_{ZL} - hc/\lambda}{kT}\right], \quad (2)$$

where k is the Boltzmann constant, T is the sample temperature, Z_l and Z_u are the partition functions of the lower and upper manifolds, respectively, and E_{ZL} is the energy difference between the lowest Stark energy level of the upper and the lower manifold (also known as the "zero-phonon line"). In general Z_l/Z_u and E_{ZL} depend on the details of the host and their exact values are not known. The published values of Z_l/Z_u range between 1 and 2 for Tm^{3+}-doped crystals[9,27,28] and E_{ZL} can be estimated from the fluorescence spectrum. Figure 4 shows the emission cross sections of Tm:phosphate obtained from Eq. (1) by using τ_{rad} from the Judd–Ofelt analysis and from Eq. (2) by using the absorption of the $^3F_4$ level. The results of the two methods are in reasonable, but not perfect, agreement. The differences might be due to reabsorption, which in Tm is not negligible due to the strong overlap of the emission and the absorption spectra, or to the uncertainties in the determination of E_{ZL} and Z_l/Z_u. Also the Judd–Ofelt method may be expected to give a less than accurate value of τ_{rad} for Tm^{3+} since only four or five peaks can be used to fit the three Judd–Ofelt parameters. Nevertheless, the relative agreement between the two results by using Eqs. (1) and (2) confirms that the radiative lifetime is of the order of a millisecond in Tm:phosphate, very different from the 50 μs fluorescence lifetime we measured near 0 K, as we will discuss later in this paper. Similar small differences between the emission cross section as calculated by using the FL and the reciprocity methods were found for Tm:germanate and Tm:silica.

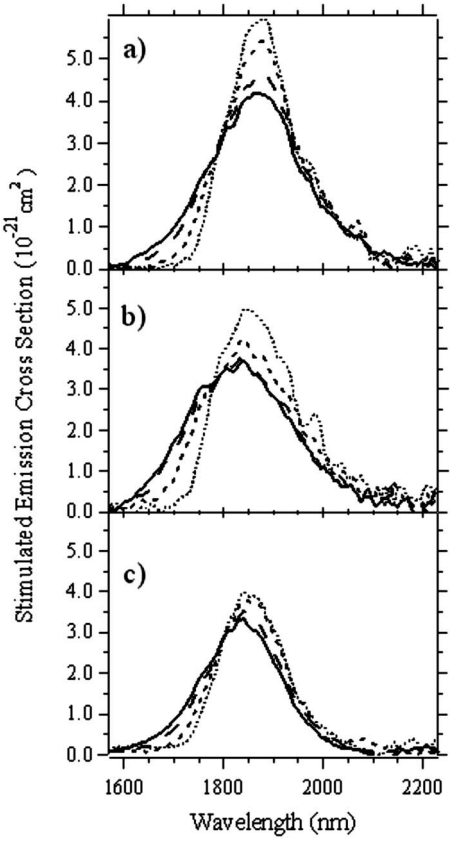

FIG. 5. Stimulated emission cross section of the $^3F_4$-$^3H_6$ transition at 35 K (···), 100 K (---), 200 K (– – –), and 295 K (——): (a) Tm:germanate, (b) Tm:silica, and (c) Tm:phosphate.

C. Temperature dependence of emission cross section

Figure 5 shows the stimulated emission cross-section spectra at different temperatures for Tm:germanate, Tm:silica, and Tm:phosphate, as obtained by using Eq. (1) and the values of τ_{rad} from the Judd–Ofelt analysis. The peak emission cross section increases when the temperature is reduced, as would be expected due to the reduction in phonon-induced peak broadening at lower temperatures. The values of the cross section around room temperature are similar in the three glasses although those of Tm:germanate seem to be slightly higher. In particular, at room temperature $\sigma_{em} \approx 4 \times 10^{-21}$ cm^2 which is in reasonable agreement with that measured by Walsh and Barnes[19] (5.8×10^{-21} cm^2), Jackson and King[29] (6×10^{-21} cm^2), and Zou and Toratani[22] in Tm:silica (6.1×10^{-21}cm^2) and by Walsh *et al.*[9] (6.8×10^{-21} cm^2) in Tm:germanate. The systematically smaller values that we obtain can be explained by the lower value for the radiative lifetime used by the earlier researchers that in turn could be

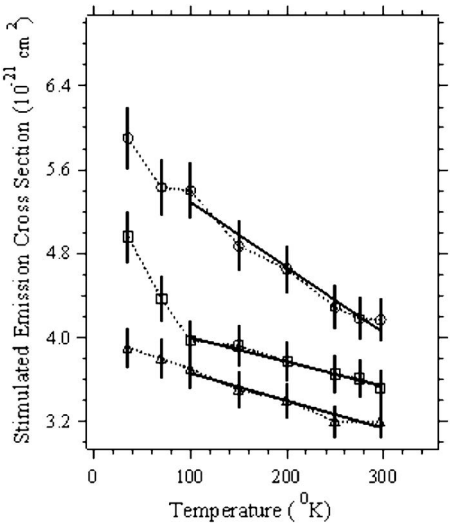

FIG. 6. Peak stimulated emission cross section as a function of the temperature for ○, Tm:germanate; □, Tm:silica; and △, Tm:phosphate. The lines are a linear fit in the 100–300 K range in each case.

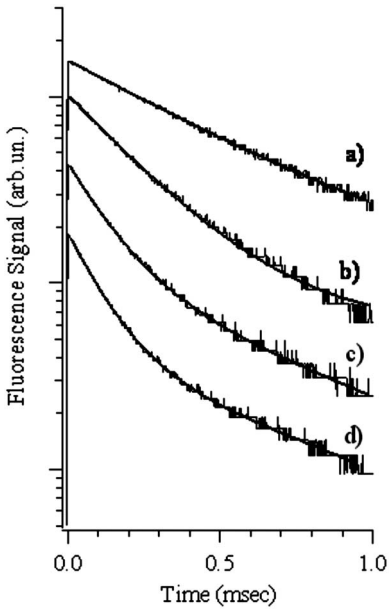

FIG. 7. The $^3F_4$-$^3H_6$ transition fluorescence decay profile of Tm:silica at (a) 35 K, (b) 100 K, (c) 200 K, and (d) 297 K: –, experimental measurement: —, best fit plot by using single exponential for (a) and (b) and double exponential for (c) and (d).

due either to the errors in applying the Judd–Ofelt analysis or to real differences in the materials investigated.

In Tm:germanate, the peak emission wavelength does not drift with temperature as it does in the other two materials. Near 1792 nm and in the 1950–2050 nm range the emission cross section is almost independent of the temperature. Also, for the other two materials the variations of cross sections in the 1900–1950 nm range are small, especially for temperatures higher than 200 K where lasers are usually operated. This feature could be used to build temperature-independent lasers around 1920 nm.

The peak emission cross section does varies with the temperature, as depicted in Fig. 6. In the 100–300 K range, the dependence is almost linear given by

$$\sigma_{em} = 5.9 \times 10^{-21}\ (\mathrm{cm}^2) - 6.2 \times 10^{-24}\ (\mathrm{cm}^2/\mathrm{K})T(\mathrm{K}) \quad (\mathrm{Tm{:}germanate}),$$

$$\sigma_{em} = 4.3 \times 10^{-21}\ (\mathrm{cm}^2) - 2.3 \times 10^{-24}\ (\mathrm{cm}^2/\mathrm{K})T(\mathrm{K}) \quad (\mathrm{Tm{:}silica}),$$

$$\sigma_{em} = 3.9 \times 10^{-21}\ (\mathrm{cm}^2) - 2.6 \times 10^{-24}\ (\mathrm{cm}^2/\mathrm{K})T(\mathrm{K}) \quad (\mathrm{Tm{:}phosphate}).$$

In the same temperature range, the peak emission wavelength varies as

$$\lambda_{em} = 1870\ \mathrm{nm} \quad (\mathrm{Tm{:}germanate}),$$

$$\lambda_{em} = 1871\ (\mathrm{nm}) - 0.21\ (\mathrm{nm/K})T(\mathrm{K}) \quad (\mathrm{Tm{:}silica}),$$

$$\lambda_{em} = 1857\ (\mathrm{nm}) - 0.07\ (\mathrm{nm/K})T(\mathrm{K}) \quad (\mathrm{Tm{:}phosphate}).$$

D. Decay dynamics

The three samples show very different decay dynamics. At room temperature the fluorescence decay time of the $^3F_4$ level is about 3 ms in germanate and is 50 μs in phosphate. Unlike Tm:germanate and Tm:phosphate the fluorescence decay profile of Tm^{3+} in silica has double exponential at room temperature (τ_{slow}=650 μs and τ_{fast}=115 μs) which turns into a single exponential pattern only at very low temperatures (Fig. 7).

The temperature dependence of the fluorescence lifetime of Tm:germanate and Tm:phosphate is depicted in panels (a) and (c) of Fig. 8. Changing the pump energy from 10 μJ/pulse to 10 mJ/pulse had no significant effect on the observed dependence. The same values of lifetime were found when the Tm:phosphate sample was pumped to the $^3H_5$ level or when the emission at 1470 nm was blocked with a filter. This confirms that the values reported in panel (c) of Fig. 8 are pertinent to the $^3F_4 \rightarrow {}^3H_6$ transition in the phosphate glass only.

The fluorescence decay lifetime τ_{fluo} is the result of the radiative and the nonradiative decay of the $^3F_4$ state, according to the formula

$$1/\tau_{fluo} = 1/\tau_{rad} + 1/\tau_{nr}. \quad (3)$$

The radiative lifetime τ_{rad} is usually independent of the temperature. On the contrary, the nonradiative lifetime τ_{nr} increases at lower temperatures although its specific dependence on temperature depends on the characteristics of the sample such as phonon energy. For many RE-doped crystals and glasses the multiphonon energy-gap law[30] applies:

$$1/\tau_{nr} \propto (1 + n(T))^p, \quad (4)$$

where p is the number of phonons of energy $h\nu$ simultaneously emitted in the decay and $n(T)$ is the Bose–Einstein factor:

$$n(T) = (e^{h\nu/kT} - 1)^{-1}. \quad (5)$$

At temperatures close to absolute zero, $1/\tau_{nr} \ll 1/\tau_{rad}$ and the measured fluorescence lifetime should be equal to the radia-

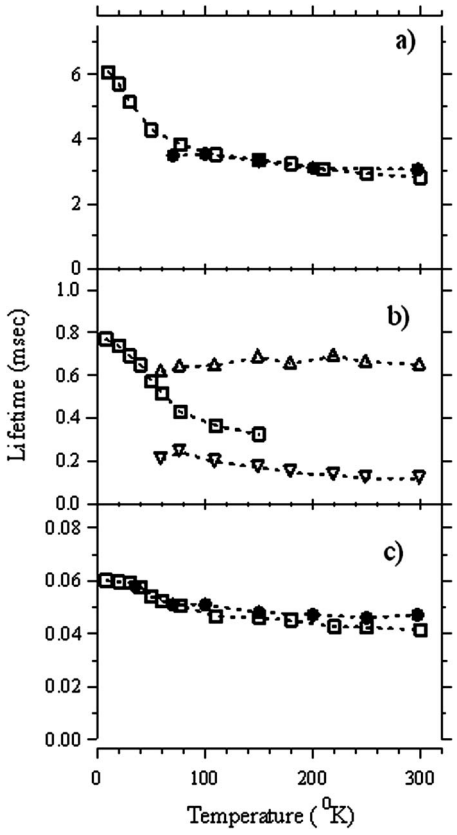

FIG. 8. The $^3F_4$-$^3H_6$ decay lifetime vs temperature: (a) Tm:germanate, (b) Tm:silica, and (c) Tm:phosphate, pumped to the $^3H_4$ level with pump energy of □ ~ 10 μJ/pulse and ● ~ 10 mJ/pulse. At high temperatures, the Tm:silica decay is characterized by a double-exponential function with a fast (▽) and a slow (△) component.

tive lifetime value obtained by the Judd–Ofelt analysis. This is the case for Tm:germanate but is clearly not for Tm:phosphate with fluorescence lifetime at 8 K two orders of magnitude lower than the value calculated by using the Judd–Ofelt analysis. However, the consistency of the emission cross section at room temperature as calculated with the reciprocity method and with the FL method by assuming the Judd–Ofelt calculated radiative lifetime (see Fig. 4 and the discussion above) supports a value of $\tau_{rad} \sim 8$ ms for Tm:phosphate. Furthermore, Eqs. (4) and (5) describe a smooth change of $\tau_{nr}(T)$ with temperatures[31–34] whereas a rapid increase can be seen in Fig. 8(b) for temperatures below 50 K. Such a rapid increase has been observed before in other Tm^{3+}-doped crystals[31,32] and glasses.[33,34] In samples with high doping concentration the nonradiative decay is significantly affected by cross relaxation, radiation trapping, and impurity quenching.[31] Also, deviations from the multiphonon energy-gap law were found when the energy difference between the upper and the lower Tm^{3+} levels is large.[33] Cornacchia *et al.*[32] developed a diffusion-limited relaxation model to explain this in which the energy of ions in the excited $^3F_4$ level migrates from ion to ion until it gets absorbed by an impurity (in their case OH^- ions). They obtained a simple analytical formula which was able to explain the temperature dependence of the fluorescence lifetime of the $^3F_4 \rightarrow {}^3H_6$ transition in Tm^{3+}:$LiLuF_4$,[32] Tm^{3+}-doped chalcogenide,[34] and sulfide[33] glass. In contrast, the $^3H_4 \rightarrow {}^3H_5$ transition in Tm^{3+}-doped silicate, phosphate, and germanate satisfies Eqs. (4) and (5).[30] A quantitative comparison of our measurements with the diffusion-limited relaxation model is very difficult due to the many parameters of that model that are unknown for the materials we investigated. Nevertheless, the general trends in Fig. 8 for the $^3F_4 \rightarrow {}^3H_6$ transition are in better agreement with the diffusion-limited model than with the multiphonon energy-gap law. Although it states a rapid increase of τ_{nr} at low temperatures the diffusion-limited model can not account for the large difference between τ_{fluo} and τ_{rad} around 8 K in Tm:phosphate.[35]

The investigation of the temperature dependence of the lifetime in Tm:silica is complicated by the nonexponential profile at temperatures above ~150 K. Deviations from a single exponential decay have been observed before in different Tm^{3+}-doped glasses.[8,36,37] Lincoln *et al.*[36] explained the fluorescence decay of Tm^{3+}:silica in terms of the strong multiphonon contribution to the decay rate. The inhomogeneous broadening of the Tm^{3+} energy levels causes a large spread of the Stark levels of the $^3H_4$, $^3H_5$, $^3F_4$, and $^3H_6$ states, resulting in different values of the energy gap for different Tm^{3+} ions within the same sample. Even small variations in the energy gap will significantly change the multiphonon decay rate. By assuming a Gaussian distribution of the energy gaps for different ions, Lincoln *et al.*[36] were able to reproduce the decay profile of the $^3H_4$ and $^3F_4$ levels by using a numerical calculation. Recently, Moulton *et al.*[38] reported a double-exponential decay in Tm-doped silica glass grown by Nufern. In a 2–2.8 wt % doped sample at room temperature they measured a fast component of $\tau_1 = 280$ μs and a slow component of $\tau_2 = 630$ μs. Unlike Lincoln *et al.*, Moulton *et al.* suggested the presence of two different optically active Tm^{3+} centers in the silica matrix to explain the nonexponential decay profile. A double exponential of the type

$$F(t) = A \exp(-t/\tau_{slow}) + B \exp(-t/\tau_{fast}) \quad (6)$$

correctly reproduces the decay profile we measured in Tm:silica for temperatures of 150 K and higher. In particular, $\tau_{slow} = 650$ μs and $\tau_{fast} = 115$ μs are obtained at room temperature and are consistent with the values of Moulton *et al.*[38] On the contrary, below 60 K the decay profile is definitely a single exponential. In the transition region between 60 and 150 K Eq. (6) can still reproduce the measured profiles better than a single exponential but because the double exponential pattern is much less pronounced the fitting procedure converges more slowly. The values of τ_{slow} and τ_{fast} returned by the fit are less accurate. For this reason, in order to extract the fluorescence lifetime Eq. (6) was used in the 60–300 K region and a single exponential was used from 8 to 150 K (bold lines in Fig. 7). The values of fluorescence lifetime of the $^3F_4$ state of Tm^{3+} in silica obtained when pumping the sample with ~10 μJ/pulse are shown in panel (b) of Fig. 8. Pumping the sample by using 10 mJ/pulse or pumping the sample to the $^3H_5$ state (at ~1200 nm) did not show any difference in the measured lifetimes. When the temperature was changed from 300 to 60 K the slow component was not significantly affected whereas the decay time associated with the fast component increased by a factor of

~2. In the interpretation of Moulton *et al.* this would mean that the quenching was stronger for the short-lived center near room temperature. Below 60 K the fluorescence lifetime shows a behavior similar to that of the other two materials investigated: A rapid increase in measured lifetime when the temperature is lowered in disagreement with the multiphonon energy-gap law. Also, as in Tm:phosphate, τ_{fluo} at 8 K is significantly lower than τ_{rad}, although the difference is now only a factor of 10.

Finally, we note that our observation of the decay profile of Tm:silica becoming a single exponential when the sample is cooled down below 60 K to reduce the phonon contribution is also consistent with the interpretation of Lincoln *et al.* Thus, the choice between the explanation of Moulton *et al.* and Lincoln *et al.* is still undecided. This and the previously mentioned difference between the radiative lifetime and the fluorescence lifetime at 8 K suggest that further investigation is necessary in order to understand the decay of the $^3F_4$ state in Tm:silica and Tm:phosphate in greater detail.

IV. CONCLUSIONS

The emission cross section of the $^3F_4 \rightarrow {}^3H_6$ transition of Tm^{3+} was measured at different temperatures in Tm^{3+}-doped silica, germanate, and phosphate glass. Although the three materials show similar values of emission cross section the much longer fluorescence lifetime of Tm:germanate makes it a more suitable material for laser purposes than the other two. Also, the peak emission wavelength in Tm:germanate does not shift with temperature and there are some wavelengths for which the emission cross section is temperature independent. Operation at these wavelengths could be used to design temperature-independent lasers. Despite the negative dn/dT and its other interesting properties, its very short fluorescence lifetime makes Tm^{3+}:phosphate a poor alternative to silica for lasing at 1870 nm. In all three materials the decay dynamics of the $^3F_4$ level significantly deviates from the multiphonon energy-gap law. Further investigation is required to understand the large difference between radiative lifetime and fluorescence lifetime near 0 K observed in Tm:phosphate as well as the nonexponential decay of Tm:silica.

ACKNOWLEDGMENTS

This work was supported by DoD JTO MRI Contract No. W911NF-05-1-0517, and the State of Florida. We also acknowledge useful conversations with Ying Chen, William Hageman, Tim McComb, and Hans P. Jenssen.

[1]G. J. Koch, M. Petros, J. Yu, and U. N. Singh, Appl. Opt. **41**, 1718 (2002).
[2]W. Koechner, *Solid State Laser Engineering*, 5th ed. (Springer-Verlag, New York, 1999).
[3]G. Armagan, A. M. Buoncristiani, and B. Di Bartolo, Opt. Mater. (Amsterdam, Neth.) **1**, 11 (1992).
[4]S. A. Brawer and W. B. White, J. Chem. Phys. **63**, 2421 (1975).
[5]D. Di Martino, L. F. Santos, A. C. Marques, and R. M. Almeida, J. Non-Cryst. Solids **293–295**, 394 (2001).
[6]R. Reisfeld, and C. K. Jorgensen, *Excited State Phenomena in Vitreous Materials* (Elsevier, Amsterdam, 1987), pp. 1–90.
[7]www.kigre.com/glass
[8]P. Jander and W. S. Brocklesby, IEEE J. Quantum Electron. **40**, 509 (2004).
[9]B. M. Walsh, N. P. Barnes, D. J. Reichle, and S. Jiang, J. Non-Cryst. Solids **352**, 5344 (2006).
[10]R. Balda, L. M. Lacha, J. Fernández, and J. M. Fernández-Navarro, Opt. Mater. (Amsterdam, Neth.) **27**, 1771 (2005).
[11]L. Meisong, Z. Junjie, H. Lili, S. Hongtao, and F. Yongzheng, Acta Opt. Sin. **26**, 713 (2006).
[12]R. Balda, J. Fernandez, A. de Pablos, J. M. F. de Navarro, and M. A. Arriandiaga, Phys. Rev. B **53**, 5181 (1996).
[13]K. Binnemans, R. Van Deun, C. Görler-Walrand, and J. L. Adam, J. Non-Cryst. Solids **238**, 11 (1998).
[14]S. A. Payne, L. L. Smith, L. K. Smith, W. L. Kway, and W. F. Krupke, IEEE J. Quantum Electron. **QE-28**, 2619 (1992).
[15]www.nufern.com
[16]www.kigre.com
[17]Kigre, personal communication (2007).
[18]B. M. Walsh, N. P. Barnes, and B. Di Bartolo, J. Appl. Phys. **83**, 2772 (1998).
[19]B. M. Walsh and N. P. Barnes, Appl. Phys. B: Lasers Opt. **78**, 325 (2004).
[20]E. Rukmini and C. K. Jayasankar, J. Non-Cryst. Solids **176**, 213 (1994).
[21]R. Reisfeld and C. K. Jorgensen, *Handbook on the Physics and Chemistry of Rare Earths*, edited by K. A. Gscheneidner, Jr. and L. Eyring (Elsevier, Amsterdam, 1987), Vol. IX, Chap. 58.
[22]X. Zou and H. Toratani, J. Non-Cryst. Solids **195**, 113 (1996).
[23]S. V. J. Lakshman, Proc. SPIE **1128**, 325 (1989).
[24]T. Komukai, T. Yamamoto, T. Sugawa, and Y. Miyajima, IEEE J. Quantum Electron. **31**, 1880 (1995).
[25]S. Aozasa, T. Sakamoto, T. Kanamori, K. Hoshino, K. Kobayashi, and M. Shimizu, IEEE Photonics Technol. Lett. **12**, 1331 (2000).
[26]E. R. Taylor, L. N. Ng, and N. P. Sessions, J. Appl. Phys. **92**, 112 (2002).
[27]V. Sudesh, J. A. Piper, and E. M. Goldys, J. Opt. Soc. Am. B **15**, 239 (1998).
[28]V. Sudesh and K. Asai, J. Opt. Soc. Am. B **20**, 1829 (2003).
[29]S. Jackson and T. A. King, J. Lightwave Technol. **17**, 948 (1999).
[30]C. B. Layne, W. H. Lowdermilk, and M. J. Weber, Phys. Rev. B **16**, 10 (1977).
[31]I. Sokólska, W. Ryba-Romanowski, S. Gołab, M. Baba, M. Świrkowicz, and T. Łukasiewicz, J. Phys. Chem. Solids **61**, 1573 (2000).
[32]F. Cornacchia, L. Palatella, A. Toncelli, M. Tonelli, A. Baraldi, R. Capelletti, E. Cavalli, K. Shimamura, and T. Fukuda, J. Phys. Chem. Solids **63**, 197 (2002).
[33]V. G. Truong, B. S. Ham, A. M. Jurdyc, B. Jacquier, J. Leperson, V. Nazabal, and J. L. Adam, Phys. Rev. B **74**, 184103 (2006).
[34]V. G. Truong, A. M. Jurdyc, B. Jacquier, B. S. Ham, A. Q. Le Quang, J. Leperson, V. Nazabal, and J. L. Adam, J. Opt. Soc. Am. B **23**, 2588 (2006).
[35]The presence of OH^- ions in the samples we investigated has been confirmed by both glass manufacturers although Nufern was not able to provide the OH^- ion concentration in Tm:silica. (Ref. 39) Kigre, Inc. estimated it to be some few parts per million (Ref. 17) in its samples. For comparison, the concentration of OH^- ions in the sample of Cornacchia *et al.* was about 40 ppm (see also Ref. 32).
[36]J. R. Lincoln, W. S. Brocklesby, F. Cusso, J. E. Townsend, A. C. Tropper, and A. Pearson, J. Lumin. **50**, 297 (1991).
[37]D. A. Simpson, G. W. Baxter, S. F. Collins, W. E. K. Gibbs, W. Blanc, B. Dussardier, and G. Monnom, J. Non-Cryst. Solids **352**, 136 (2006).
[38]E. Slobodtchikov, P. F. Moulton, and G. Frith, Efficient, High-Power, Tm-Doped Silica Fiber Laser, 20th Solid State Diode Laser Technology Review, 26–28 June, Los Angeles, CA, 2007 (unpublished).
[39]Nufern, personal communication (2007).